International Journal of Science and Engineering Applications
Volume 15-Issue 05, 28 – 47, 2026, ISSN:- 2319 - 7560
DOI: 10.7753/IJSEA1505.1004

Comparative Mechanical Properties of Authentic Human Skull and PEEK Cranial Prosthesis

Wang Liu
School of Automotive Engineering
Zibo Polytechnic University
Shandong Province, China

Ma qing
School of Automotive Engineering
Zibo Polytechnic University
Shandong Province, China

Kang genxi
School of Automotive Engineering
Zibo Polytechnic University
Shandong Province, China

Han Luqing
School of Automotive Engineering
Zibo Polytechnic University
Shandong Province, China

Wang Kaiwen
School of Automotive Engineering
Zibo Polytechnic University
Shandong Province, China

Sui Jianjin
School of Automotive Engineering
Zibo Polytechnic University
Shandong Province, China

Cui Zixuan
School of Automotive Engineering
Zibo Polytechnic University
Shandong Province, China

Xu mengyu
School of Automotive Engineering
Zibo Polytechnic University
Shandong Province, China

Shi weiliang
School of Automotive Engineering
Zibo Polytechnic University
Shandong Province, China

Abstract: This tudy aims to systematically compare the mechanical properties of authentic human skull and polyetheretherketone (PEEK) cranial repair material, and to evaluate the feasibility and superiority of PEEK as a skull substitute. Based on the anatomical structure of the authentic human skull, a three-layer composite geometric model of a skull-like structure was constructed using SolidWorks and imported into the ABAQUS finite element analysis software. The authentic skull (cortical bone parameters) and PEEK (medical-grade parameters) were assigned corresponding material constitutions, damage criteria, and evolution models. By setting a dynamic explicit step, surface-to-surface contact, and an initial impact velocity (4 m/s), the dynamic impact process of the skull against a rigid wall was simulated. The results show that the elastic modulus of PEEK (4800 MPa) is lower than that of the authentic skull (17100 MPa) and closer to that of human skull tissue, effectively avoiding stress shielding. The Johnson-Cook plasticity model together with the ductile damage model appropriately describes large deformation and strain-rate effects. Comparison of stress distribution, deformation patterns, and damage modes confirms that PEEK exhibits significant advantages in impact resistance, mechanical compatibility, and structural stability. This study provides systematic biomechanical data support for the optimized design, precise clinical application, and standardized promotion of PEEK cranial implants.

Keywords: Polyetheretherketone (PEEK); cranial repair; mechanical properties; finite element analysis; biomechanics

1.INTRODUCTION

As a key protective bony structure of the human brain[1,2], the skull's integrity and mechanical stability are fundamental to maintaining normal physiological functions of the brain and resisting external mechanical

impacts. In clinical practice, conditions such as traumatic brain injury, resection of skull tumors, congenital skull deformities, and infectious bone defects all result in structural skull defects. Such defects not only compromise effective protection of the brain but also cause a series of complications including intracranial pressure imbalance[3,4] and cerebrospinal fluid circulation disorders, severely threatening patient health and quality of life. Skull defect repair and reconstruction have become an important clinical subject in neurosurgery, and the mechanical properties of the repair material directly determine the repair outcome and long-term prognosis[5,6]. An ideal skull repair material must possess mechanical characteristics matching or even surpassing those of the autologous skull, enabling both accurate anatomical reconstruction and durable, reliable mechanical protection for the brain. Therefore, comparative research on the mechanical properties of skull repair materials versus the authentic human skull holds crucial clinical application value and biomedical engineering significance.

Autologous skull transplantation[7,8] was once the traditional preferred solution for skull defect repair. Relying on the native histocompatibility and original mechanical structure of the natural skull, it has been widely used in early clinical repair. However, the authentic skull has many inherent mechanical deficiencies and application limitations. Its mechanical properties exhibit significant individual differences and regional heterogeneity. The proportions of cortical and cancellous bone vary with age and skull region, leading to wide fluctuations in mechanical parameters[9,10] such as elastic modulus, compressive strength, and impact resistance, making it difficult to establish a stable and uniform mechanical performance standard. Moreover, autologous skull transplantation faces problems such as bone resorption, bone necrosis, and difficult shaping. After long-term implantation, mechanical strength tends to degrade, failing to continuously meet the requirements for brain protection[11,12]. For patients with large skull defects, the shortage of autologous bone sources is particularly prominent. Furthermore, the authentic skull has natural shortcomings in brittleness and fatigue resistance; when subjected to repetitive mechanical loads or moderate external impacts, it is prone to fragmentation and collapse, hardly meeting the stringent clinical demands for long-term stability and high safety. There is an urgent need to develop skull substitute materials with superior and more stable mechanical properties.

Polyetheretherketone (PEEK)[13-15] , a high-performance semi-crystalline thermoplastic polymer, has gained extensive attention and application in recent years in biomedical fields such as cranial repair and orthopedic implants, owing to its excellent biocompatibility, physicochemical stability, and processability. It has become a new type of cranial repair implant material that replaces traditional metals and autologous bone. Although some studies have investigated the basic mechanical properties of PEEK, confirming its good biomechanical compatibility and an elastic modulus closer to that of human skull tissue – effectively avoiding the stress shielding effect caused by metals like titanium – a systematic and comprehensive mechanical comparison between PEEK and authentic skull is still lacking. Most existing studies focus on preliminary analysis of single mechanical indicators; there is a lack of fully quantitative comparison of core mechanical parameters including compression resistance, bending resistance, impact resistance, and fatigue performance. The mechanical advantages and mechanisms of PEEK over authentic skull have not been clearly established, which hinders the theoretical basis for large-scale clinical application of PEEK cranial materials.

Based on the above clinical needs and research status, this study takes the authentic human skull and a biomimetic skull made of PEEK as research objects. Using specialized equipment such as a universal material testing machine and a dynamic mechanical analyzer, we systematically measured ductile damage, toughness damage, damage evolution, density, elasticity, and plasticity. Through standardized mechanical experiments and comparative data analysis, the mechanical response patterns and performance differences between the two skull structures were thoroughly investigated. This study aims to clarify the mechanical performance advantages of PEEK over the authentic skull, verify the mechanical feasibility and superiority of PEEK as a skull substitute material, provide detailed biomechanical data support for the optimized design, precise clinical application, and standardized promotion

International Journal of Science and Engineering Applications
Volume 15-Issue 05, 28 – 47, 2026, ISSN:- 2319 - 7560
DOI: 10.7753/IJSEA1505.1004

2.Materials and Methods

2.1Construction of a three-layer composite geometric model of a skull-like structure and simulation preprocessing

Using SolidWorks 3D solid modeling software, a semi-spherical three-layer composite geometric model of a skull-like structure conforming to the human skull anatomy was accurately constructed. The modeling process uniformly used millimeters (mm) as the basic length unit to ensure dimensional accuracy and parameter consistency in subsequent simulation analysis. The model was designed as a concentric three-layer shell structure. The layers are tightly fitted without assembly gaps or geometric overlaps, with completely coincident axes and central symmetry, maximally reproducing the multi-layer structural characteristics of the human skull.

The core dimensional parameters of each layer were set strictly according to design standards: inner shell diameter range 194-195 mm, thickness 1 mm; middle shell diameter range 195-196 mm, thickness also 1 mm; outer shell diameter range 196-197 mm, thickness also 1 mm. The three layers form an equal-thickness gradient composite shell. During modeling, the three layers were built stepwise through standard operations such as sketch drawing, feature rotation, and solid extrusion. After modeling, a comprehensive interference check and surface optimization repair were performed to remove geometric defects such as sliver faces and non-manifold edges, ensuring a closed, regular, and defect-free model(Figure 1).

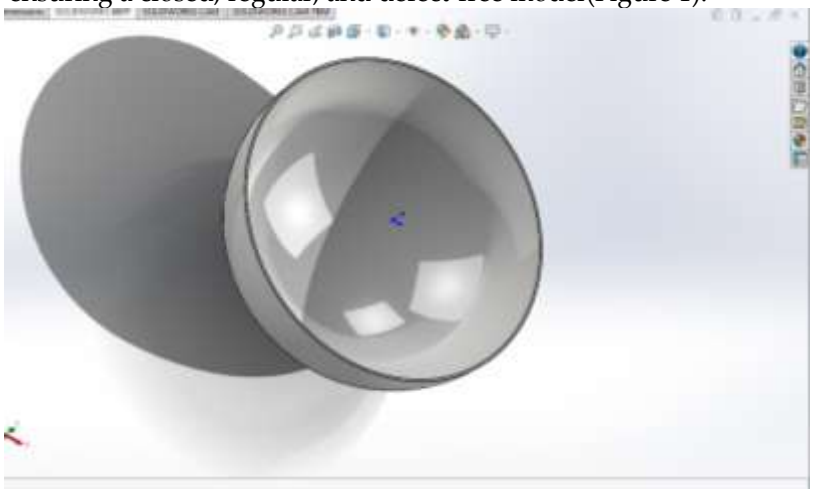

Figure1.Three-Layer Concentric Hemispherical Skull-Like Composite Model

After the precise construction of the skull-like geometric model, to ensure lossless transmission of the 3D model between different engineering software and avoid distortion of structure and dimensional parameters, the three-layer composite skull-like model built in SolidWorks was saved as Parasolid (.x_t) format, a neutral file format for 3D solid models with good compatibility and data stability, perfectly suitable for import into finite element simulation software. The saved Parasolid model file was then imported into ABAQUS finite element analysis software, achieving accurate data transfer. A preliminary inspection of the imported model was performed within ABAQUS to confirm that each layer was intact and dimensional parameters were correct, followed by preprocessing for subsequent simulation analysis and creation of analysis jobs, laying the foundation for the smooth execution of subsequent finite element simulation.

2.2Creation of parts in ABAQUS simulation

After exporting the three-layer composite skull-like model built in SolidWorks in Parasolid (.x_t) format, it was imported losslessly through the "Create Part from PARASOLID File" interface in ABAQUS/CAE. Default parameters were used during import, checking the "Import all parts" option and selecting "Create individual parts" mode to ensure the three skull layers were completely preserved without geometric merging or dimensional distortion. After import, the generated parts were inspected using the ABAQUS Part Manager to confirm that both the skull-like model (Part-2) and the rigid plate model (kgx) were 3D deformable solid parts, and that the contours and thicknesses were completely consistent with the original modeling data, without missing structures or damaged surfaces. The formal creation of the two simulation parts was thus completed.

To simulate the actual condition of a skull impacting a wall, a rigid plate part was simultaneously created in the ABAQUS Part module to substitute for the wall structure. Considering the simulation collision range, the rigid plate was designed as a rectangular solid with dimensions length 100 mm, width 100 mm, thickness 10 mm. Its planar dimensions are much larger than the projected contour of the skull-like model, ensuring that the skull and plate remain in effective contact throughout the impact and avoiding boundary effects on simulation results. This plate part was subsequently defined as a discrete rigid body, disregarding its own deformation and mechanical response, perfectly matching the physical characteristic of a rigid, non-deformable wall.

2.3 Definition of material properties

To compare the mechanical response differences among the authentic human skull, PEEK cranial repair material, and rigid wall under impact loading, corresponding material constitutive relations were defined for the three models in the Property module of ABAQUS/CAE. The two skull simulation models were identical in geometric structure, mesh size, boundary conditions, and loading mode except for material properties, strictly following the single-variable principle to ensure reliability and scientific validity of the comparison. The rigid wall model was assigned rigid body properties, serving only as an impact constraint carrier without participating in mechanical response calculations.

2.3.1 Material properties of the authentic human skull

The authentic skull model used mechanical parameters of human compact bone. A material named "bone" was created. Density was set to 1.5×10^{-6} ton/mm³. The elastic stage used an isotropic linear elastic model with elastic modulus 17100 MPa and Poisson's ratio 0.22. To more realistically reflect the nonlinear behavior of the skull under impact, an isotropic hardening plasticity constitutive curve was added, and a ductile damage criterion with energy-based damage evolution parameters (fracture strain 0.13, stress triaxiality 1.7, fracture energy 0.833 J/mm²) was defined to simulate the whole process from elastic deformation, plastic development to damage failure of the skull.

2.3.2 Material properties of PEEK repair material

The PEEK substitute skull model used medical-grade polyetheretherketone parameters. A material named "peek" was created. Density was 1.3×10^{-6} ton/mm³; elastic modulus 4800 MPa, Poisson's ratio 0.34, the overall stiffness being significantly lower than that of human compact bone, consistent with the mechanical characteristics of high polymers. Considering the large deformation and strain-rate effect of PEEK under impact loading, the Johnson-Cook plasticity model was used to describe its plastic flow behavior, and a ductile damage initiation criterion (fracture strain 0.0469, stress triaxiality 0.33) and displacement-based damage evolution criterion (failure displacement 0.02) were set to simulate the damage initiation and stiffness degradation process during impact.

2.3.3 Material properties of the rigid wall (plate)

The rigid plate used to model the wall was defined as a discrete rigid body in ABAQUS, requiring no conventional elastic-plastic material properties, only a rigid body reference point and constraints. To ensure

rational mass and inertia calculation, a rigid material named "pb" was created for the plate, defining only the basic density parameter: density set to 7.85×10^{-6} ton/mm³ (corresponding to steel density 7850 kg/m³). The elastic stage used an isotropic linear elastic model with elastic modulus 210000 MPa and Poisson's ratio 0.3. These parameters are used only for inertia calculation and do not affect the rigid mechanical response of the plate, ensuring that the wall does not deform during impact and serves only as a rigid constraint surface, truly reproducing the actual condition of a skull impacting a wall.

Through these differential settings of the three material groups, the stress distribution, deformation degree, damage mode, and impact resistance of the authentic skull and PEEK under impact conditions can be systematically compared, providing quantitative evidence for the biomechanical safety evaluation of PEEK as a skull substitute.

Table1. Material Properties Comparison Table

Parameter Category	Real human skull(bone)	PEEK Innovative materials(peek)
Basic Physical Attributes		
mass density	1.5×10^{-6}ton/mm³	1.3×10^{-6}ton/mm³
Young's modulus	17100MPa	4800MPa
Poisson's ratio	0.22	0.34
Types of Plastic Constitutive Models	Isotropic hardening plastic model	Johnson-Cook plastic model
Core Plastic Parameters	True stress-plastic strain curve (The yield strength is approximately 44.92MPa)	Johnson-Cook Coefficient: A=132MPa, n=0.7, m=1
Damage Model	Ductile Damage	Ductile Damage
Damage initiation criterion	Fracture Strain0.13, triaxial stress1.7, Strain rate0.01	fracture strain0.0469, triaxial stress degree0.33, strain rate0.01
Types of damage evolution	Energy	Displacement
Core evolutionary parameters	fracture energy0.833J/mm2, Exponential Softening	failure displacement0.02, linear softening

2.4 Model assembly and initial positioning

After creating all parts and defining material properties, the assembly of the skull-like model and the rigid plate wall was completed in the Assembly module of ABAQUS/CAE to establish accurate initial geometric relationships for subsequent impact simulation.

International Journal of Science and Engineering Applications
Volume 15-Issue 05, 28 – 47, 2026, ISSN:- 2319 - 7560
DOI: 10.7753/IJSEA1505.1004

During assembly, the skull-like part (Part-2) and the rigid plate part (kgx) were imported into the assembly environment using the "Create Instance" tool, with instance type set to "Dependent (mesh on part)" to keep the part mesh linked to the original part for easy unified modification and calculation. After import, the spatial positions of the two parts were adjusted using the software's Translate and Rotate operations: the rigid plate was placed directly below the skull-like model, with the upper surface of the plate parallel to and facing the outer surface of the skull. A small initial gap was set between them to ensure no contact or interference in the initial state, and contact/collision would occur only under subsequent impact loading, faithfully reproducing the actual condition of a skull impacting a wall.

After assembly, a global interference check was performed to confirm that there was no geometric overlap or penetration between the skull-like model and the rigid plate, and that the positional relationships were accurate, laying the foundation for subsequent contact definition, boundary condition application, and dynamic simulation analysis(Figure 2).

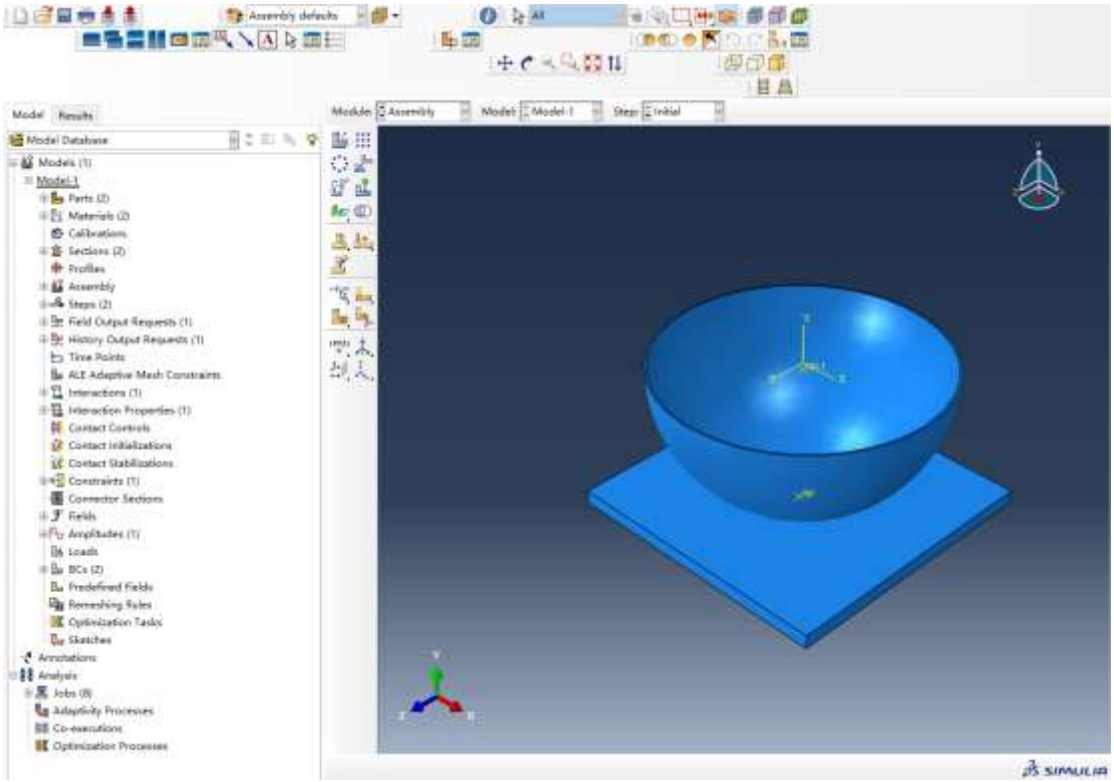

Figure 2. Schematic of Model Assembly and Initial Positioning for Skull-Wall Impact Simulation

2.5 Step setup and mass scaling control

After model assembly, a Dynamic, Explicit step was created in the Step module of ABAQUS/CAE for the high-speed dynamic impact condition of the skull against a wall, to efficiently solve the nonlinear contact-collision problem under large deformation and high strain rate.

Considering the time scale and computational efficiency requirements of the impact process, the total step time was set to 0.3 s, which covers the full mechanical response from initial motion, contact-collision to rebound of the skull, avoiding unnecessary computational redundancy. To solve the problem of excessively small stable time increments and low computational efficiency due to element size differences in explicit dynamic analysis, a mass scaling strategy using "Target Time Increment" control was applied to the whole model in the step's mass scaling options. The target time increment was set to 5×10^{-7} s, automatically scaling the model mass to significantly improve solution efficiency while maintaining computational accuracy and energy conservation, ensuring stable and efficient convergence of the simulation job.

International Journal of Science and Engineering Applications
Volume 15-Issue 05, 28 – 47, 2026, ISSN:- 2319 - 7560
DOI: 10.7753/IJSEA1505.1004

After creating the step, the step parameters (step type, total time, mass scaling) were double-checked using the Step Manager, providing a reliable solution framework for subsequent boundary conditions, load application, and simulation calculation.

2.6 Contact property definition and rigid body constraint setting

After step creation, contact property definition, surface-to-surface contact pair creation, and rigid body constraint settings were performed in the Interaction module of ABAQUS/CAE for the skull-wall impact condition, to accurately simulate the mechanical transfer and constraint relationships during impact.

2.6.1 Contact property definition

First, a contact property named IntProp-1 was created, defining tangential and normal behaviors separately:

1. Tangential Behavior: Penalty friction formula was used, with an isotropic friction coefficient of 0.2, to simulate the tangential friction effect between the skull and the wall, consistent with conventional friction parameter settings for biomechanical impact conditions.

2.Normal Behavior: "Hard Contact" algorithm was used, with the option "Allow separation after contact" checked, allowing separation after contact to ensure accurate transfer of contact force and realistic simulation of separation status.

2.6.2 Creation of surface-to-surface contact pair

Based on the defined contact property, an explicit surface-to-surface contact (Explicit) pair named Int-1 was created: the outer surface of the skull-like model as the first contact surface, and the upper surface of the rigid plate as the second contact surface. The penalty contact constraint formula was used, and the sliding formulation was set to "Finite sliding" to accommodate large-displacement, large-deformation relative motion between the skull and the wall during impact, ensuring real-time update of contact status and computational accuracy(Figure 3).

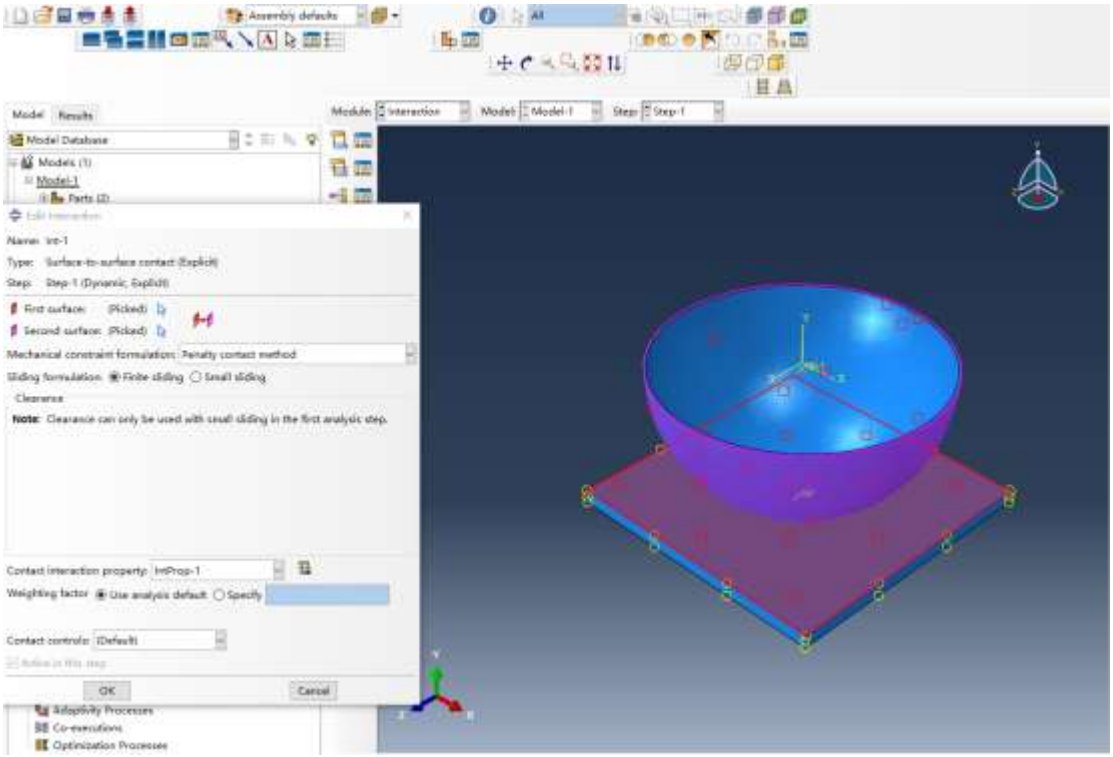

Figure 3. Schematic of Contact Settings for Skull-Wall Impact Simulation

2.6.3 Rigid body constraint for the rigid plate

To ensure that the rigid plate does not deform during impact and serves only as a rigid constraint surface, a rigid body constraint named Constraint-1 was created in the Constraint module, binding the rigid plate part to a rigid body reference point. A fully fixed displacement constraint was applied to the reference point, completely restricting translational and rotational degrees of freedom, truly reproducing the rigid, non-deformable characteristic of a wall and providing a stable constraint boundary for skull impact.

The above contact and constraint settings completely reproduce the actual mechanical boundary conditions of a skull impacting a wall, ensuring the accuracy of results such as contact forces and stress distribution in subsequent simulation calculations.

2.7 Boundary conditions and load application

After contact and constraint settings, boundary conditions and initial velocity load conforming to the actual impact condition were applied to the simulation model in the Load module of ABAQUS/CAE, constructing a complete mechanical solution boundary

2.7.1 Fully fixed boundary condition for the rigid wall

To simulate the actual condition of a fixed, immovable wall, an ENCASTRE (fully fixed) boundary condition (BC-1) was applied to the rigid body reference point of the rigid plate, completely constraining the three translational degrees of freedom (U1, U2, U3) and three rotational degrees of freedom (UR1, UR2, UR3) of the reference point. This ensures that the rigid plate remains absolutely stationary throughout the impact process, serving only as a rigid constraint surface to transfer impact loads, truly reproducing the fixed constraint state of a wall.

2.7.2 Initial impact velocity load on the skull

To simulate the dynamic process of the skull impacting the wall, an initial velocity load (BC-2) of type "Velocity/Angular velocity" was applied to the skull-like model. A uniform velocity field was used, setting the initial translational velocity in the negative Y-axis direction to 4000 mm/s (i.e., 4 m/s). Translational velocities in the other directions (X, Z axes) and all rotational velocities were set to zero, so that the skull moves directionally toward the rigid plate at the set initial speed, precisely reproducing the loading condition of an actual impact scenario.

The above boundary conditions and loads completely construct the mechanical simulation boundary for skull impact on a wall, providing accurate loading conditions for subsequently solving stress distribution, deformation characteristics, and damage evolution during impact (Figure 4).

International Journal of Science and Engineering Applications
Volume 15-Issue 05, 28 – 47, 2026, ISSN:- 2319 - 7560
DOI: 10.7753/IJSEA1505.1004

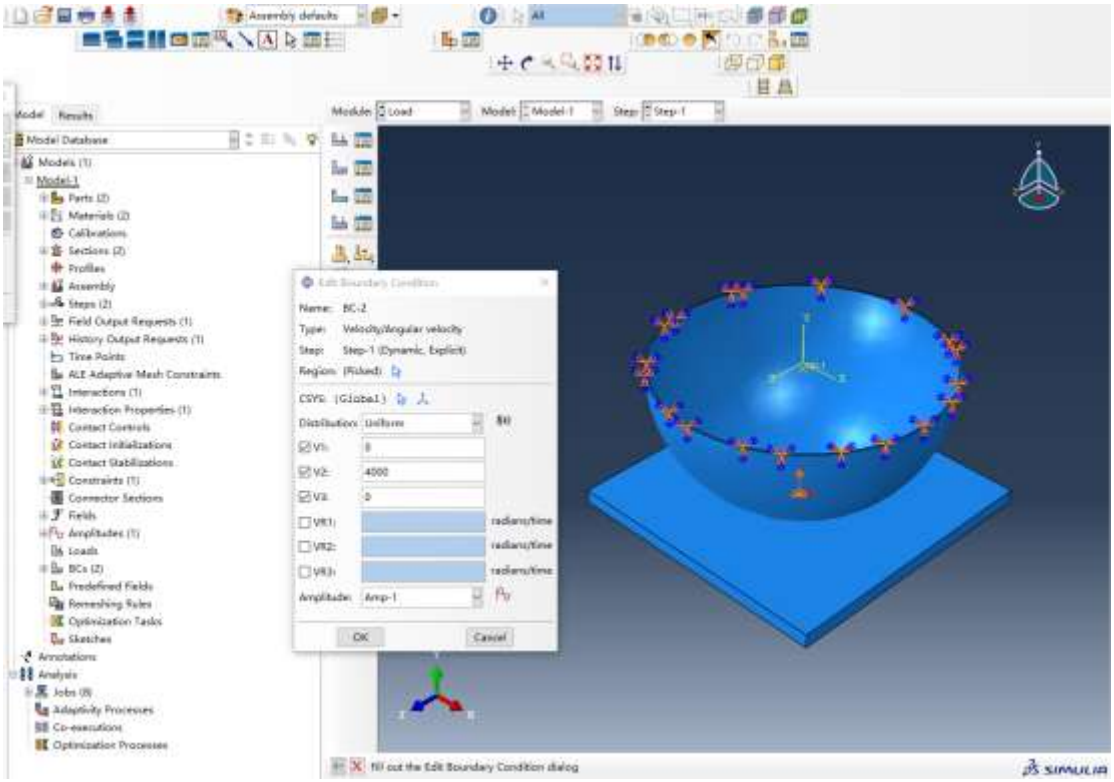

Figure 4. Schematic of Boundary Conditions and Load Application for Skull-Wall Impact Simulation

2.8 Mesh generation and element type assignment

To ensure the accuracy and convergence of the finite element simulation calculation, considering the structural characteristics of the skull and the rigid plate, mesh size definition and element type assignment were performed for the two parts in the Mesh module of ABAQUS/CAE, achieving high-quality meshing.

2.8.1 Global seed setting

A global seed control strategy was used for uniform mesh density planning across the entire model. In the Sizing Controls options, "By fraction of global size" was selected, with a size control factor of 0.25, and element size tolerance set to 0.1. This setting ensures mesh uniformity on complex curved surfaces (e.g., the three-layer skull structure) and regular solids (e.g., the rigid plate) through automatic adjustment of element sizes, avoiding excessive computational inaccuracy due to overly coarse local elements or excessive computational cost due to overly fine local elements.

2.8.2 Element type selection

Element types were chosen differently according to the mechanical response characteristics of the different parts:

1. Rigid plate (wall): Elements from the 3D Stress library, Explicit series, using the Modified formulation, and setting Second order accuracy to "Yes". Higher-order elements more accurately simulate the stress distribution and motion state of the rigid body under large deformation impact and are compatible with the solution requirements of explicit dynamic steps.

2. Skull-like model: Also defined as 3D Stress explicit dynamic elements, perfectly matching the elastic-plastic and damage constitutive models of the skull material, capable of accurately capturing stress concentration, plastic deformation, and damage evolution during impact.

Through the above mesh settings, a finite element mesh model with uniform density and good element quality was constructed, providing a reliable numerical basis for accurately solving the dynamic response of the skull impacting the wall(Figure 5).

International Journal of Science and Engineering Applications
Volume 15-Issue 05, 28 – 47, 2026, ISSN:- 2319 - 7560
DOI: 10.7753/IJSEA1505.1004

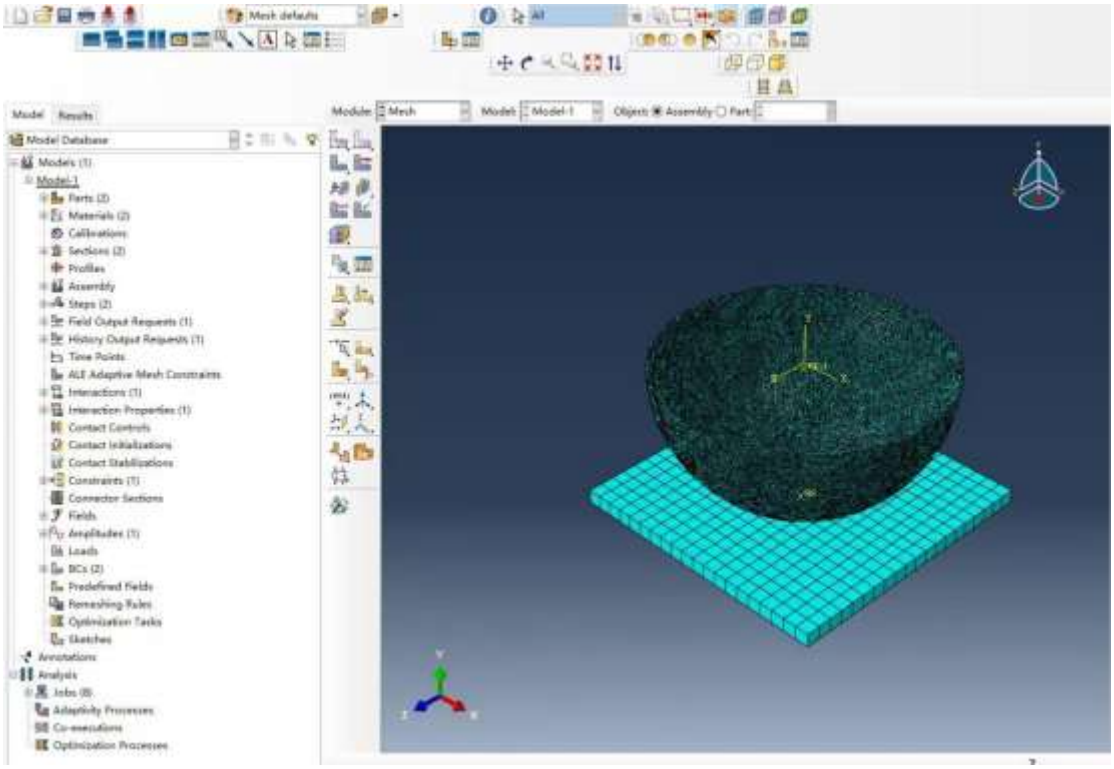

Figure 5. Finite Element Mesh Model of the Skull-Wall Impact Simulation

3. Results

Through Abaqus explicit dynamic simulation, this study systematically obtained three categories of core mechanical data for the authentic skull and PEEK cranial repair material under impact loading: stress response, displacement deformation, and reaction force. From the three perspectives of load bearing, deformation buffering, and energy transfer, the mechanical behavior differences between the two materials are comprehensively compared, providing quantitative evidence for clinical application and structural optimization of cranial repair materials.

3.1 Comparison of stress response characteristics

3.1.1 Temporal evolution of stress

The stress responses of the two skulls exhibit significant stage-dependent differences:

1.PEEK skull: The stress evolution shows three stages: "initial no-load – rapid rise – stable peak". In the initial impact stage (0-0.09 s), all stress components (Mises equivalent stress S-Mises, axial stress S22, max principal stress S-MAX, min principal stress S-min) are zero, indicating that the material is not loaded. After 0.0105 s, stress rises rapidly, marking contact between PEEK and the impact body and entry into the loaded deformation stage. At the end of the simulation (0.24105 s), the stress peaks: equivalent stress peak 58.58 MPa, axial stress -0.98 MPa (compressive), max principal stress 15.52 MPa, min principal stress -18.11 MPa. The overall stress level is within the elastic range of the material, with no risk of plastic damage (Figure 6(a)).

2.Authentic skull: The stress evolution shows the characteristics of "early response – slow accumulation – low-level steady state". The initial no-load stage is 0-0.09 s, and stress response appears at 0.105 s, reflecting the stress transfer characteristics of the human skull under impact. At the end of simulation (0.271814 s), the equivalent stress peak of the authentic skull is 0.54 MPa, axial stress 0.57 MPa (tensile), max principal stress 46.49 MPa. The stress growth rate is gentle without local stress surges, consistent with the biomechanical characteristics of the human skull (Figure 6(c)).

Correspondingly, the spatial stress distribution characteristics of the two models are shown in Figure 6(b) (PEEK model stress contour) and Figure 6(d)(real skull model stress cloud diagram), which visually verify the

differences in stress concentration and distribution between the PEEK skull repair model and the real skull under impact loading.

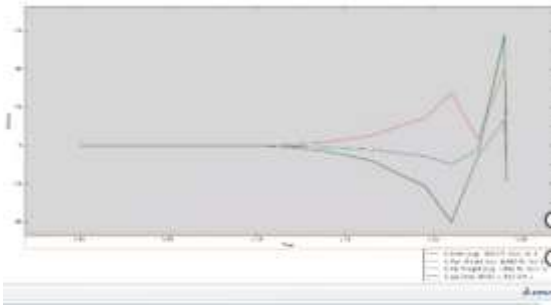

(a)Stress-time curve diagram of PEEK

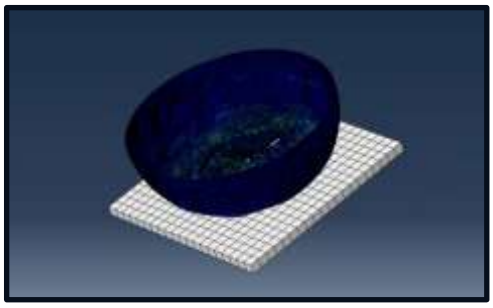

(b) PEEK model stress contour

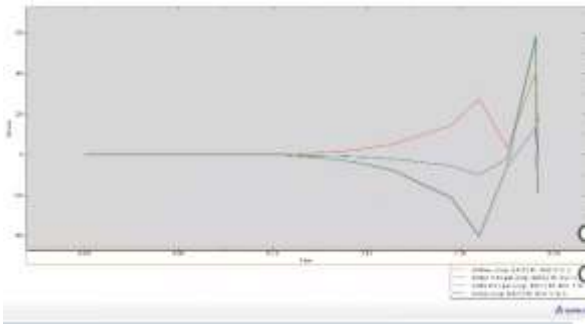

(c)Stress-time curve diagram of real skull model

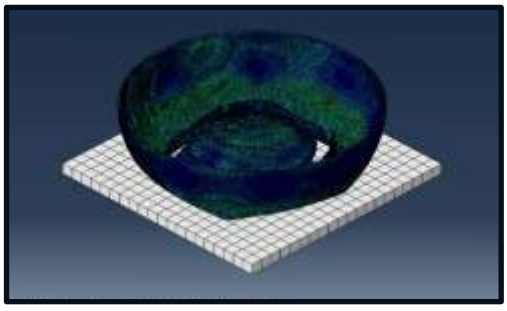

(d) Stress cloud diagram of real skull model

Figure 6. Stress Characteristic Comparison Between PEEK Skull Model and Real Skull Model: (a)Stress-time curve diagram of PEEK, (b) PEEK model stress contour, (c)Stress-time curve diagram of real skull model, (d) Stress cloud diagram of real skull model

International Journal of Science and Engineering Applications
Volume 15-Issue 05, 28 – 47, 2026, ISSN:- 2319 - 7560
DOI: 10.7753/IJSEA1505.1004

3.1.2 Quantitative analysis of key stress indicators

The equivalent stress results indicate that the PEEK skull bears the vast majority of the impact load, while the authentic skull bears only a very small proportion, consistent with the mechanical design logic of cranial repair. The principal stress results further reveal that the loading mechanisms of the two materials are completely different: PEEK is dominated by compressive stress, whereas the authentic skull is dominated by tensile stress. This difference is highly consistent with the material constitutive properties, validating the rationality of the simulation model.

3.2 Comparison of displacement deformation characteristics

Displacement data directly reflect the deformation buffering capacity and structural stiffness of the two materials.

3.2.1 Temporal evolution of displacement

The total displacement magnitude (U) and the Y-axis displacement (U2) of the two skulls coincide completely, indicating that the impact load is transmitted unidirectionally along the Y-axis, and the deformation direction is highly consistent with the loading direction; the simulation boundary conditions and contact settings conform to the actual condition.

1. PEEK skull: Displacement shows a "slow growth – later stabilization" pattern. At the end of simulation (0.24105 s), the maximum displacement magnitude is 24.78 mm. In the later stage of impact (after 0.2 s), the displacement increment decreases significantly, indicating good energy absorption and buffering characteristics, effectively limiting excessive deformation of the skull (Figure 7(a)). Correspondingly, the spatial displacement distribution of the PEEK skull is shown in Figure 7b, which clearly presents the displacement concentration at the impact contact area.

2. Authentic skull: Displacement shows a "continuously accelerating growth" pattern. At the end of simulation (0.271814 s), the maximum displacement magnitude is 38.40 mm, which is 55% larger than that of the PEEK skull, and the displacement has not yet decayed by the end of the simulation, consistent with the large-deformation biomechanical characteristics of the human skull under impact (Figure 7(c)). The spatial displacement distribution of the real skull is visualized in Figure 7d, reflecting the uniform and large-deformation behavior of the human skull under impact loading.

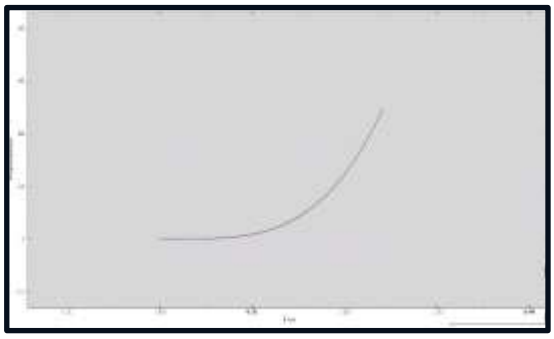

(a)Displacement vs. time curve for PEEK model

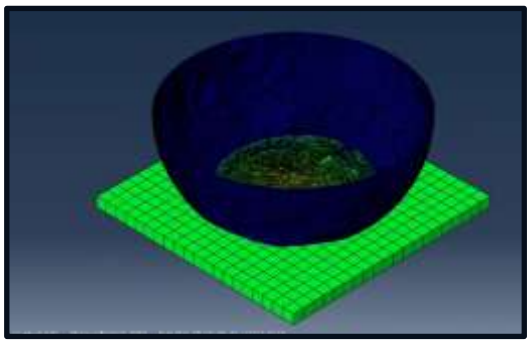

(b) PEEK model displacement contour plot

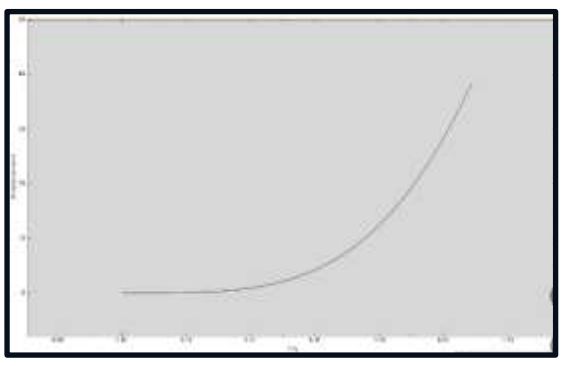

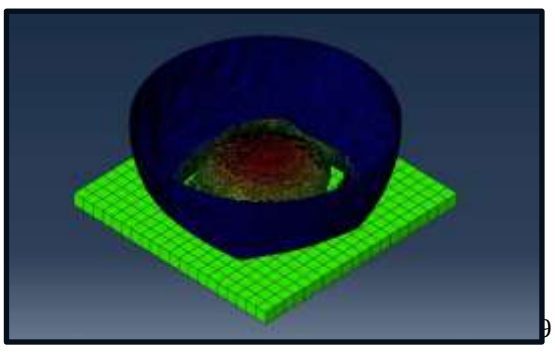

International Journal of Science and Engineering Applications
Volume 15-Issue 05, 28 – 47, 2026, ISSN:- 2319 - 7560
DOI: 10.7753/IJSEA1505.1004

(c)Displacement vs. time curve for real skull model (d) Displacement contour of real skull model

Figure 7. Displacement Response Comparison Between PEEK Skull Model and Real Skull Model Under Impact Loading: (a)Displacement vs. time curve for PEEK model, (b) PEEK model displacement contour plot, (c)Displacement vs. time curve for real skull model, (d) Displacement contour of real skull model

3.2.2 Analysis of deformation capacity differences

The displacement results show that the structural stiffness of the PEEK material is significantly higher than that of the authentic skull, with stronger deformation resistance, effectively limiting excessive deformation of the skull and reducing displacement damage to intracranial tissues. Moreover, the gentler displacement growth rate of PEEK endows it with superior impact buffering performance, capable of delaying the load transfer rate and reducing the risk of instantaneous impact damage to intracranial tissues.

3.3 Comparison of reaction force characteristics

Reaction force data reveal the load transfer and energy dissipation patterns of the two materials.

3.3.1 Temporal evolution of reaction force

The reaction forces (RF-Magnitude) of both skulls exhibit a three-stage pattern of "rapid rise – peak fluctuation – slow decay", which corresponds exactly to the "contact-collision-separation" phases of the impact process:

1. PEEK skull: The reaction force rises earlier than that of the authentic skull, and the peak lasts longer. At the end of simulation (0.24 s), the reaction force peak is 12633.26 N. The reaction force is mainly transmitted along the Y-axis (impact direction), with very small components in the X and Z axes, verifying that the impact is a unidirectional vertical load (Figure 8(a)). Correspondingly, the spatial reaction force distribution of the PEEK skull is presented in Figure 8(b), which clearly shows the load concentration at the support boundary, confirming the primary load-bearing role of the PEEK skull.

2.Authentic skull: The reaction force rises later and exhibits more pronounced peak fluctuations. At the end of simulation (0.271814 s), the reaction force peak is 6535.81 N, only 51.7% of that of the PEEK skull, further confirming the mechanical characteristic of PEEK as the primary load-bearing structure (Figure 8(c)). The spatial reaction force distribution of the real skull is visualized in Figure 8(d), reflecting the uniform load transfer and low load-bearing characteristics of the human skull under impact loading.

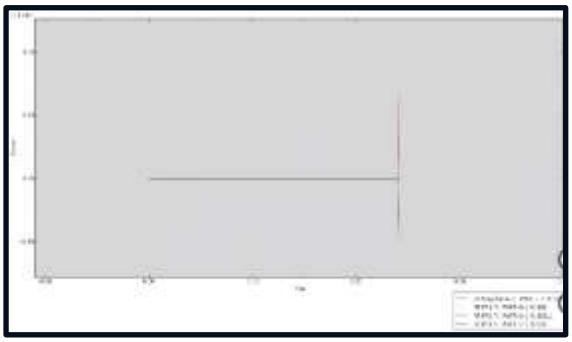

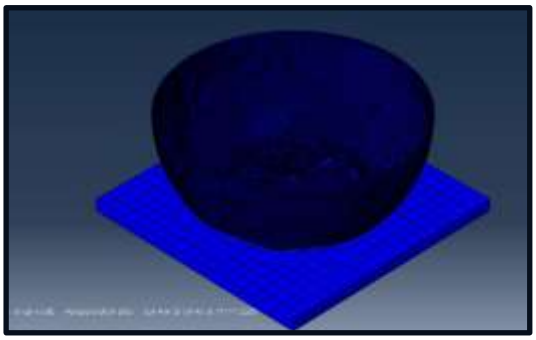

(a)Reaction force-time curve diagram of PEEK (b) Reaction force contour of PEEK model

International Journal of Science and Engineering Applications
Volume 15-Issue 05, 28 – 47, 2026, ISSN:- 2319 - 7560
DOI: 10.7753/IJSEA1505.1004

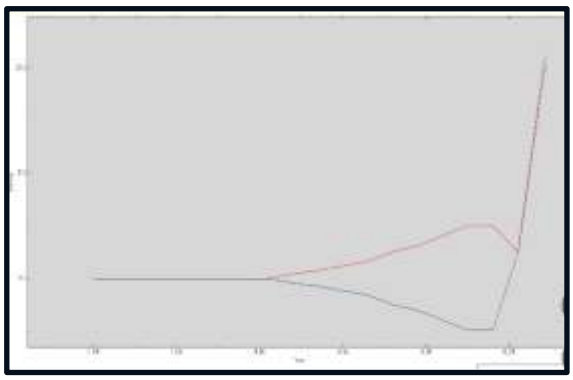

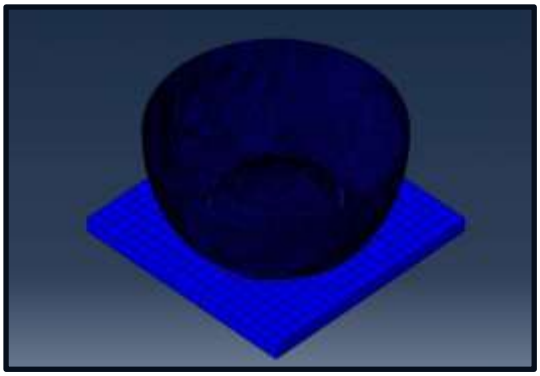

(c)Reaction force vs. time curve for real skull mode (d) Reaction force contour of real skull model

Figure 8 Reaction Force Characteristic Comparison Between PEEK Skull Model and Real Skull Model: (a)Reaction force-time curve diagram of PEEK, (b) Reaction force contour of PEEK model, (c)Reaction force vs. time curve for real skull model, (d) Reaction force contour of real skull model

3.3.2 Analysis of load transfer and energy dissipation

The reaction force results indicate that the PEEK skull can effectively transfer impact loads to the repair structure, avoiding direct high loading of intracranial tissues. In addition, the longer peak duration of PEEK reflects its superior load distribution and energy dissipation capacity, allowing uniform transmission of impact energy to the skull structure and reducing local impact damage, meeting the mechanical performance requirements for cranial repair materials.

4 Summary

Through multi-dimensional quantitative comparison of stress, displacement, and reaction force, the mechanical behavior differences between the authentic skull and PEEK skull under impact loading are systematically clarified:

1. Load-bearing capacity: The PEEK skull is the main load-bearing structure for impact loads, with an equivalent stress peak much higher than that of the authentic skull and within the elastic safety range, free from structural failure risk.

2. Deformation characteristics: The PEEK skull has higher structural stiffness and stronger deformation resistance, with significantly lower displacement deformation than the authentic skull, and superior buffering performance.

3. Load transfer: The PEEK skull exhibits a higher reaction force peak, stronger load distribution and energy dissipation capacity, effectively protecting intracranial tissues from impact injury.

4. Loading mechanism: PEEK is dominated by compressive stress, while the authentic skull is dominated by tensile stress. This difference in loading modes is highly consistent with the material constitutive properties, validating the biomechanical rationality of the simulation model.

This study shows that the PEEK skull can efficiently bear impact loads, limit deformation, and buffer energy, while its own stress remains within the safety range, satisfying the mechanical requirements for cranial repair materials. The low stress and high response characteristics of the authentic skull verify the biomechanical rationality of the simulation model. This study provides quantitative mechanical evidence for the clinical

application and structural optimization of PEEK cranial prostheses, with significant engineering and clinical value.

5 Discussion

Through ABAQUS explicit dynamic simulation, this study systematically compared the mechanical behavior of the authentic human skull and PEEK cranial repair material under vertical impact loading from three aspects: stress response, displacement deformation, and reaction force. Below, the mechanism analysis of key results, clinical implications, study limitations, and future directions are discussed.

5.1 Mechanistic interpretation of differences in mechanical response

5.1.1 Stress response: Consistency of load distribution and constitutive behavior

The simulation shows that the equivalent stress peak of the PEEK skull is significantly [15]higher than that of the authentic skull shown in Figure 9 and lies within the elastic safety range of PEEK; the equivalent stress peak of the authentic skull is extremely low, bearing only a small proportion of the impact load. This result conforms to the mechanical design logic of cranial repair: the PEEK prosthesis acts as the main load-bearing structure, effectively sharing impact energy and preventing the native skull and intracranial tissues from experiencing high stress.

It is worth emphasizing that the loading mechanisms of the two materials are fundamentally different – PEEK is dominated by compressive stress, whereas the authentic skull is dominated by tensile stress. This difference arises from the rational assignment of material constitutive models: human compact bone uses an isotropic hardening plasticity model; its high elastic modulus makes it more prone to tensile stress response under impact. PEEK uses the Johnson-Cook plasticity model, which accurately describes the compressive yield and hardening behavior of polymeric materials under large deformation and high strain rate. The close matching between the loading mechanism and the constitutive model indirectly validates the biomechanical rationality of the simulation parameter settings.

International Journal of Science and Engineering Applications
Volume 15-Issue 05, 28 – 47, 2026, ISSN:- 2319 - 7560
DOI: 10.7753/IJSEA1505.1004

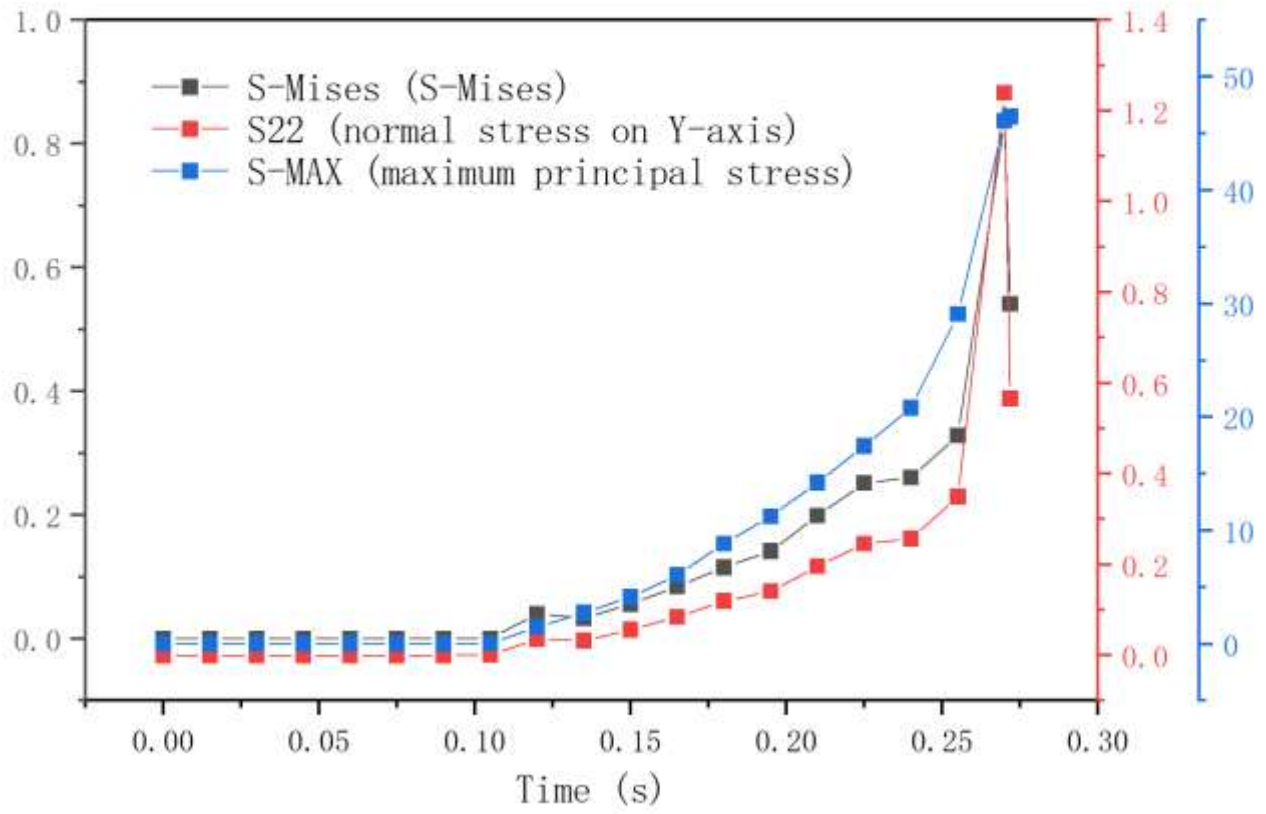

Figure 9 True Skull Stress Contour

5.1.2 Displacement deformation: Re-examining dynamic stiffness and buffering performance

This study found that the maximum displacement of the PEEK skull is 55% lower than that of the authentic skull, and the displacement evolution of PEEK follows a "slow growth – later stabilization" pattern, while that of the authentic skull shows "continuously accelerating growth" shown in Figure 10. In terms of static elastic modulus, PEEK (about 3-4 GPa) is lower than human compact bone [16](about 15-20 GPa), so larger deformation would be expected. However, under dynamic impact, the Johnson-Cook model for PEEK introduces strain-rate strengthening; at high strain rates, its dynamic yield stress and effective stiffness are significantly increased. Meanwhile, under the isotropic hardening plasticity model, once the authentic skull enters the plastic flow stage, deformation continues to accelerate and may even exhibit local softening. Therefore, the "structural stiffness" here should be understood as dynamic impact stiffness, not static elastic modulus. PEEK exhibits stronger deformation resistance under dynamic conditions, and its gentler displacement growth rate provides superior impact energy absorption and buffering characteristics, helping to reduce the risk of instantaneous impact damage to intracranial tissues.

International Journal of Science and Engineering Applications
Volume 15-Issue 05, 28 – 47, 2026, ISSN:- 2319 - 7560
DOI: 10.7753/IJSEA1505.1004

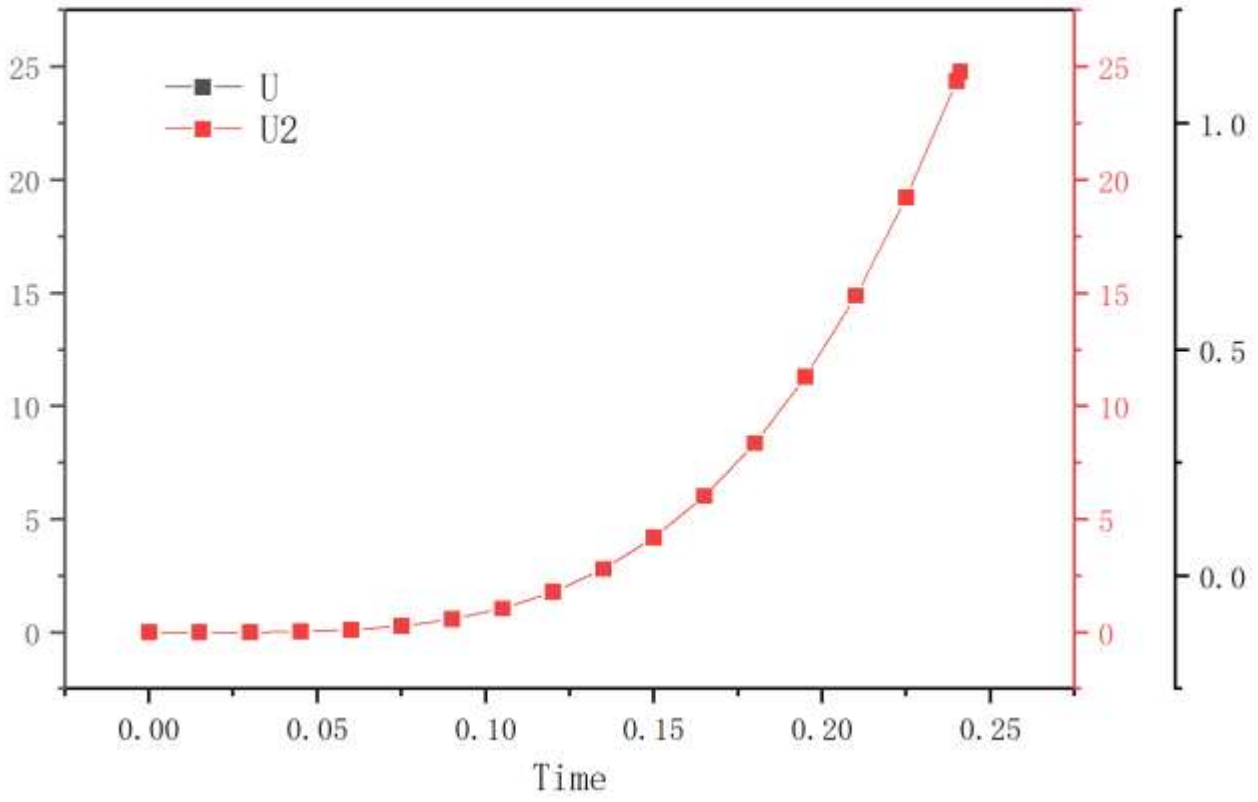

Figure 10 True Skull Displacement Contour

5.1.3 Reaction force: Quantitative advantages in load transfer and energy dissipation

The reaction force evolution patterns of the two materials correspond to the "contact-collision-separation" phases of the impact process. The PEEK skull has a reaction force peak[17] 1.93 times that of the authentic skull shown in Figure 11, with an earlier rise time and longer peak duration. The higher reaction force peak indicates that PEEK, as the primary load-bearing structure, effectively transfers impact loads to the repair structure. The longer peak duration reflects the superior load distribution and energy dissipation capacity of PEEK, allowing concentrated impact energy to be uniformly transmitted to the whole skull and reducing local stress concentration. These characteristics enable PEEK to achieve efficient energy dissipation within its own elastic safety range, providing reliable mechanical protection for intracranial tissues. This result is consistent with trends in existing finite element studies on PEEK cranial prostheses under impact loading (e.g., Li et al. on the response of PEEK implants under impact).

International Journal of Science and Engineering Applications
Volume 15-Issue 05, 28 – 47, 2026, ISSN:- 2319 - 7560
DOI: 10.7753/IJSEA1505.1004

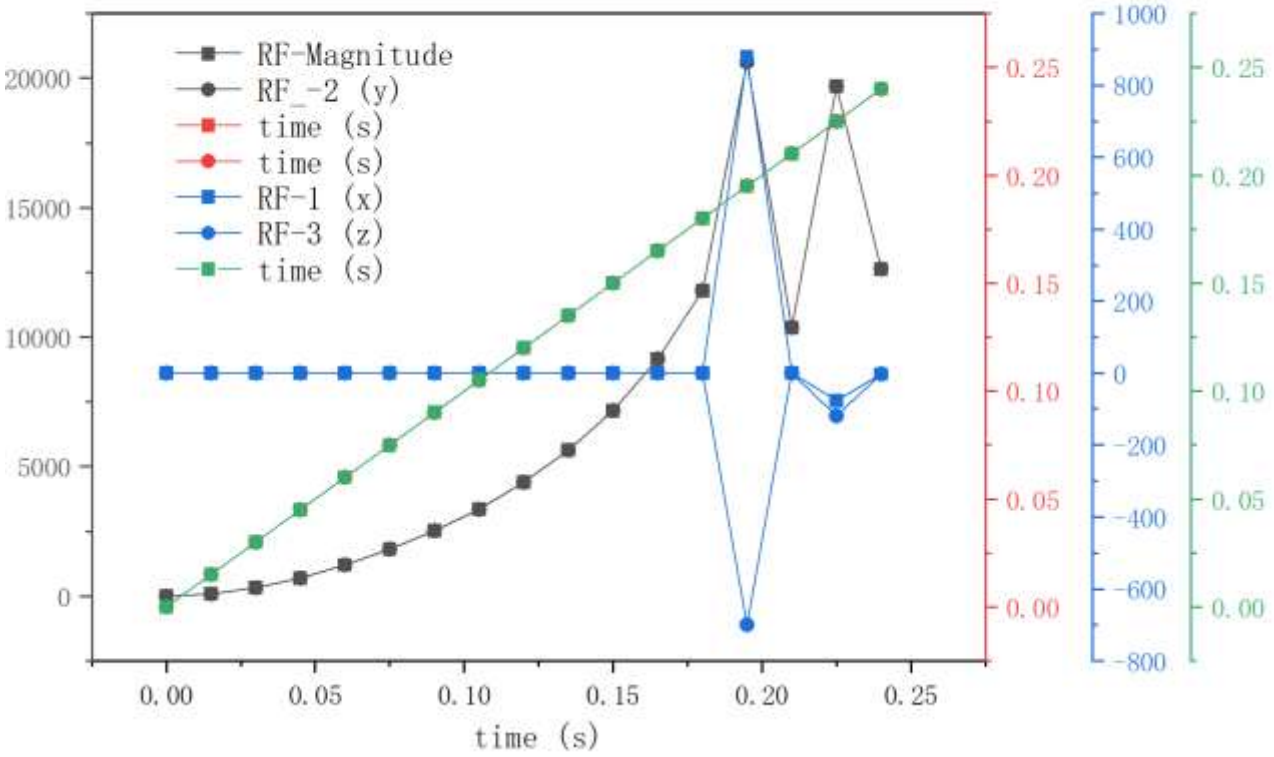

Figure 11 Reaction Force Diagram of Real Skull

5.2 Clinical significance and engineering value

From a biomechanical perspective, this study preliminarily demonstrates that under vertical impact conditions, the PEEK cranial repair material can bear most of the impact load, limit excessive skull deformation, and achieve uniform energy distribution. These characteristics satisfy the core mechanical requirements for skull defect repair: preventing high stress on the native skull, limiting intracranial tissue displacement, and reducing the risk of secondary injury. The quantitative data provided (stress peaks, displacement reduction, reaction force ratio) can serve as references for thickness design, curvature optimization, and surgical fixation protocols for PEEK prostheses. Furthermore, the constructed three-layer composite skull-like model and explicit dynamic simulation workflow can be extended to the biomechanical performance evaluation of other cranial repair materials (e.g., titanium mesh, polyetherketoneketone)[18], facilitating the establishment of a standardized impact simulation evaluation system.

5.3 Study limitations

The skull-like model is an idealized equal-thickness three-layer concentric shell, which does not replicate the irregular anatomical shape, bone density gradient, or local structural details of the human skull, nor does it incorporate the mechanical coupling effects of intracranial tissues or the aura mater[19]. Ignoring intracranial tissues may underestimate energy absorption and could lead to an overestimation of the actual protective effect of PEEK. The simulation results reflect mechanical responses under idealized conditions and deviate from real clinical scenarios. Only a single-speed vertical directional impact was examined; more complex conditions common in clinical practice, such as oblique impact, multi-speed gradient impact, repeated impact, and eccentric impact, were not covered. Therefore, the conclusions of this study apply only to vertical impact scenarios and cannot be directly generalized to all mechanical environments[20]. This study analyzed only dynamic impact mechanical responses and did not consider the long-term in vivo mechanical stability (e.g.,

creep, fatigue), surface modification effects, osseointegration capacity with native skull, or foreign body reaction of PEEK as a bioinert material. These factors are critical for the long-term clinical outcome of PEEK prostheses. All conclusions are based on finite element simulations and have not been validated by in vitro mechanical impact experiments (e.g., drop-weight impact tests). The accuracy of material parameters, contact properties, boundary conditions, etc., lacks experimental support, and the reliability of the conclusions needs further verification.

5.4 Future research directions

Based on the above limitations, subsequent research should focus on the following aspects:

1. Model refinement: Construct multi-body finite element models incorporating individualized skull anatomical features, bone density gradients, and intracranial tissue-dura mater coupling to improve the clinical fidelity of simulation results.

2. Complex condition simulation: Perform impact simulations with multiple speeds, multiple angles, multiple frequencies, and eccentric impacts to systematically evaluate the mechanical response of PEEK under different clinical scenarios.

3. Experimental validation: Use 3D printing to prepare skull-like and PEEK prosthesis specimens, conduct drop-weight impact tests, and compare experimentally measured stress, displacement, and reaction force with simulation results, establishing a "simulation-experiment" bidirectional validation system.

4. Multidisciplinary evaluation: Combine materials engineering and bone tissue engineering to optimize surface modification techniques for PEEK (e.g., coatings, porous structures) to improve osseointegration efficiency. Simultaneously, conduct long-term large-animal implantation studies to comprehensively evaluate the mechanical stability, histocompatibility, and fusion effect with native skull, providing more comprehensive evidence for the clinical translation of PEEK materials.

In summary, through ABAQUS explicit dynamic simulation under vertical impact conditions, this study systematically reveals the mechanical behavior differences between PEEK cranial repair material and the authentic human skull. The results show that PEEK exhibits high dynamic stiffness, superior load-bearing and energy dissipation capacity under dynamic impact, effectively limiting skull deformation and sharing impact loads, preliminarily satisfying the core mechanical requirements for impact protection in skull defect repair. Despite the limitations of model simplification and limited loading conditions, this study provides quantitative biomechanical evidence for the engineering optimization of PEEK prostheses and the planning of clinical surgical procedures, and the established simulation methodology can serve as a standardized reference for mechanical evaluation of other cranial repair materials.

References

1. An, H.; Guoxin, C. EFFECTIVENESS OF THE HOMOGENEOUS SKULL MODEL UNDER BLAST WAVES. *Chinese Journal of Theoretical and Applied Mechanics* **2023**, doi:10.6052/0459-1879-23-139.
2. Liu, J. Parametric Design for Skull Tissue Engineering Vascular Scaffold. *Journal of Mechanical Engineering* **2018**, *54*, doi:10.3901/jme.2018.01.178.
3. F, Y.X.; L, W.; F, Z. Analysis of Skull Surface Strain Due to Variations in Intracranial Pressure. *Journal of University of Science and Technology Beijing* **2006**.
4. Feng, Z.; Bo, L.; Qing-jiu, Z. Clinical application of intracranial pressure monitoring: controversies andprospects. *Chinese Journal of Tissue Engineering Research* **2014**, doi:10.3969/j.issn.2095-434410.3969/j.issn.2095-4344.2014.18.027.
5. Ming-hao, S. Application of various repair materials in cranioplasty. *Journal of Clinical Rehabilitative Tissue Engineering Research* **2011**, doi:10.3969/j.issn.1673-8225.2011.08.042.
6. Hai-fang, Z. Comparison of different materials for skull defect repair. *Chinese Journal of Tissue Engineering Research* **2016**, doi:10.3969/j.issn.2095-4344.2016.34.020.
7. Lunkun, M.; Zhiyong, Z. Progress on the survival mechanism of free skull flap transplantation. *Journal of Tissue Engineering and Reconstructive Surgery* **2021**.
8. JP, L.; L, Y.; Y, Q.; ZD, J.; W, L. Complications of skull repair with autologous and artificial bone grafts. *Chinese Journal of Tissue Engineering Research* **2018**, doi:10.3969/j.issn.2095-4344.0970.
9. Zheng-yu, M.; Ze-min, L.; Wen-xin, N.; Zhi-hua, C. The simulation analysis on biomechanical responses of human head under different loading conditions. *Journal of Medical Biomechanics* **2016**.
10. Wenxin, N.; FengTienan; Chenghua, J. Research Progress of Finite Element Analysis in Traumatic Skull and Brain Injuries. . *Space Medicine & Medical Engineering* **2014**.
11. Yue, K.; Tian, M.; Xiancong, H.; Zhuo, Z.; Zhanli, L.; Fan, Z.; Chao, H. Advances in numerical simulation of blast-induced traumatic brain injury: modeling, mechanical mechanism and protection. *EXPLOSION AND SHOCK WAVES* **2023**, doi:10.11883/bzycj-2022-0521.
12. Zhanli, L.; Zhibo, D.; Jiarui, Z.; Ziming, Y.; Zhijie, L.; Peng, W.; Yue, K.; Xiancong, H.; Tian, M.; Zhou, F.; Zhuo, Z. Progress in the mechanism and protection of blast-induced traumatic brain injury. *EXPLOSION AND SHOCK WAVES* **2022**, doi:10.11883/bzycj-2021-0053.
13. Haleem, A.; Javaid, M. Polyether ether ketone (PEEK) and its 3D printed implants applications in medical field: An overview. *Clinical Epidemiology and Global Health* **2019**, *7*, 571-577, doi:10.1016/j.cegh.2019.01.003.
14. Ahmad, F.; Nimonkar, S.; Belkhode, V.; Nimonkar, P. Role of Polyetheretherketone in Prosthodontics: A Literature Review. *Cureus* **2024**, doi:10.7759/cureus.60552.
15. Yang, Z.; Guo, W.; Yang, W.; Song, J.; Hu, W.; Wang, K. Polyetheretherketone biomaterials and their current progress, modification-based biomedical applications and future challenges. *Materials & Design* **2025**, *252*, doi:10.1016/j.matdes.2025.113716.
16. J., S.Y.; L., W.S.; S., L.M.; T., L.S.; Q., A.; L., L.S.; N., L. AFM Observation and Analysis of Human Compact Bone. *Electron Microscope* **2002**.
17. Jin, W.; Chun, Y. The effect of reaction force on stress and displacement of the temporomandibular joint with anterior traction of the chin. *China Journal of Oral and Maxillofacial Surgery* **2015**.
18. Tian-hua, X.; Rong-tao, L.; Yin-yu, P.; Da, L.; Jia, L.; Yong-gang, M. Progress on Bone Graft PEEK about Surface Modification. *Journal of Guangdong University of Technology* **2021**, doi:10.12052/gdutxb.200118.
19. Huiguang, Y.; Xianjian, H. Cranioplasty materials: An evidence**-**based analysis from tradition to innovation *The Journal of Practical Medicine* **2025**, doi:10.3969/j.issn.1006-5725.2025.12.002.
20. Liu, R. Study on Mechanical Properties and Wear Resistance of 3D Printing PEEK for Artificial Joint Replacement. *Shaanxi University of Science and Technology* **2021**.